Nozik, A. J. Multiple exciton generation in semiconductor quantum dots. Chem. Phys. Lett. 457, 3–11

ARTICLE *in* CHEMICAL PHYSICS LETTERS · MAY 2008

Impact Factor: 1.9 · DOI: 10.1016/j.cplett.2008.03.094

1 AUTHOR:

A. J. Nozik
University of Colorado Boulder
310 PUBLICATIONS **19,501** CITATIONS

SEE PROFILE

Chemical Physics Letters 457 (2008) 3–11

Contents lists available at ScienceDirect

Chemical Physics Letters

journal homepage: www.elsevier.com/locate/cplett

FRONTIERS ARTICLE

Multiple exciton generation in semiconductor quantum dots

Arthur J. Nozik *

National Renewable Energy Laboratory, Golden, CO 80401, USA
Department of Chemistry and Biochemistry, University of Colorado, Boulder, CO 80309, USA

ARTICLE INFO

Article history:
Received 30 January 2008
In final form 25 March 2008
Available online 7 April 2008

ABSTRACT

A review is presented of recent work on (1) the origin of the concept of enhanced multiple electron–hole pair (i.e. exciton) production in semiconductor quantum dots (QDs), (2) various experiments based on time-resolved fs to ns spectroscopy (transient IR absorption, transient visible to near-IR bleaching due to state filling, terahertz spectroscopy, and time-resolved photoluminescence) that support the occurrence of highly efficient multiple exciton generation (MEG) in QDs, (3) thermodynamic analyses of the theoretical enhancement of the conversion efficiency in solar cells that are based on MEG in QDs, (4) MEG in QD arrays that can be used in QD solar cells, (5) theoretical models to explain MEG, and (6) some recent controversy about the evidence for MEG.

1. Introduction

The efficient formation of more than one photoinduced electron–hole (e^-–h^+) pair upon the absorption of a single photon is a process not only of great current scientific interest, but is potentially important for optoelectronic devices (photovoltaic and photoelectrochemical cells) that directly convert solar radiant energy into electricity or stored chemical potential in solar-derived fuels like hydrogen, alcohols, and hydrocarbons. This is because this process is one way to improve the efficiency of the direct conversion of solar irradiance to electricity or fuel (a process we term solar photoconversion). Conversion efficiency increases because the excess kinetic energy of electrons and holes produced in a photoconversion cell by absorption of photons with energies above the threshold energy for absorption (the bandgap in semiconductors and the HOMO–LUMO energy difference in molecular systems) creates additional e^-–h^+ pairs when the photon energy is at least twice the bandgap or HOMO–LUMO energy, and the extra electrons and holes can be separated, transported, and collected to yield higher photocurrents in the cell. In present photoconversion cells such excess kinetic energy is converted to heat and becomes unavailable for conversion to electrical or chemical free energy, thus limiting the maximum thermodynamic conversion efficiency. Since at present the most prevalent form of photoconversion cells are photovoltaic (PV) cells that generate solar electricity, we will only discuss these types of cells here. However, the fundamental principles of the topics we present here are the same for cells that produce either electricity or fuel; the difference lies in the engineering design of the two types of cells, and those differences are presented elsewhere [1,2].

The creation of more than one e^-–h^+ pair per absorbed photon has been recognized for over 50 years in bulk semiconductors; it has been observed in the photocurrent of bulk p–n junctions in Si, Ge, PbS, PbSe, PbTe, and InSb [3–10], and in these systems is termed impact ionization. However, impact ionization in bulk semiconductors is not an efficient process and the threshold photon energy required is many multiples of the threshold absorption energy. For important PV semiconductors like Si, which is overwhelming dominant in the photovoltaic cells in use today, this means that impact ionization does not become significant until the incident photon energy exceeds 3.5 eV, an ultraviolet energy threshold that is beyond the photon energies present in the solar spectrum. Furthermore, even with 5 eV photons, impact ionization only generates a quantum yield of about 1.3. Hence, impact ionization in bulk semiconductors is not a meaningful approach to increase the efficiency of conventional PV cells.

However, for semiconductor nanocrystals (also called quantum dots (QDs)) the generation of multiple e^-–h+ pairs from a single photon becomes very efficient and the threshold photon energy for the process to generate two electron–hole pairs per photon can approach values as low as twice the threshold energy for absorption (the absolute minimum to satisfy energy conservation); this effect allows the threshold to occur in the visible or near-IR spectral region.

In semiconductor QDs, the e^-–h^+ pairs become correlated because of the spatial confinement and thus exist as excitons. Therefore, we label the formation of multiple excitons in quantum dots multiple exciton generation (MEG); other authors prefer to use the term carrier multiplication (CM). However, since free charge carriers do not exist in isolated QDs and they can only form upon dissociation of the excitons and subsequent separation of the electrons and holes in a device architecture, we prefer to use the former term and will do so here.

* Fax: +1 303 384 6655.
E-mail address: arthur_nozik@nrel.gov

0009-2614/$ - see front matter © 2008 Elsevier B.V. All rights reserved.
doi:10.1016/j.cplett.2008.03.094

In this review, the reasons why MEG in QDs is much more efficient and has a lower photon energy threshold than does impaction ionization in bulk semiconductors will be explained, experimental evidence for MEG in PbSe, PbS, PbTe, and Si QDs will be presented, theoretical models for the mechanism of MEG will be discussed, and we will also discuss experiments to observe MEG in photocurrent extracted from QDs in various cell configurations. Finally, we will discuss some recent controversial issues about MEG in QDs.

2. Theoretical thermodynamic conversion efficiency of radiant energy to free energy

We start our review with a discussion of the maximum thermodynamic limits of the solar power conversion efficiency in PV cells based on conventional bulk semiconductors where one e^-–h^+ pair per absorbed photon is produced, and for cases where multiple e^-–h^+ pairs per photon are created. This difference provides the incentive to investigate MEG in QDs and in solar cells based on QDs.

2.1. PV with bulk semiconductors

The maximum thermodynamic efficiency for the conversion of unconcentrated solar irradiance into electrical free energy in a single-threshold bulk absorber was calculated by Shockley and Queisser in 1961 [11] to be about 31%; the analysis is also valid for the conversion to chemical free energy [12,13]. This calculation was based on several constraints: (1) the only loss of photogenerated electrons and positive holes (charge carriers) is through radiative recombination (this is termed the radiative limit); (2) detailed balance is assumed; (3) a maximum yield of one e^-–h^+ pair per absorbed photon is produced; and (4) thermal equilibrium is attained between electrons and phonons. The 31% maximum efficiency value is achieved in semiconductors with bandgaps ranging from about 1.2 to 1.4 eV. The solar spectrum contains photons with energies ranging from about 0.5 to 3.5 eV, so photons with energies below the optimum bandgap are not absorbed, while those with energies above it create electrons and holes with a total excess kinetic energy equal to the difference between the photon energy and the bandgap. For a Boltzmann ensemble of the photogenerated carriers, this excess kinetic energy creates an effective temperature that can be much higher than the lattice temperature; such charge carriers are termed 'hot electrons and hot holes' and the initial carrier temperature upon photon absorption can be as high as 10 times a lattice temperature of 300 K. In bulk semiconductors, the division of this kinetic energy between electrons and holes is determined by their effective masses, with the carrier having the lower effective mass receiving more of the excess energy [14].

In the Shockley–Queisser analysis, the biggest loss factor limiting the conversion efficiency to 31% is that the absorbed photon energy above the semiconductor bandgap is lost as heat through electron–phonon scattering and subsequent phonon emission, as the carriers relax to their respective bandedges (bottom of conduction band for electrons and top of valence band for holes) and equilibrate with the phonons (see Fig. 1). The present approach to reduce this loss and increase efficiency above the 31% limit has been to use a stack of cascaded multiple p–n junctions with descending bandgap values along the direction of the incident light such that higher energy photons are absorbed in the higher bandgap semiconductors and lower energy photons in the lower bandgap semiconductors; this reduces the overall heat loss due to carrier relaxation via phonon emission. Such cells are generally called tandem solar cells. In the limit of an infinite stack of bandgaps perfectly matched to the solar spectrum in a tandem cell, the ultimate conversion efficiency at one-sun intensity increases to about 66%. Actual efficiencies of about 32% have been reported

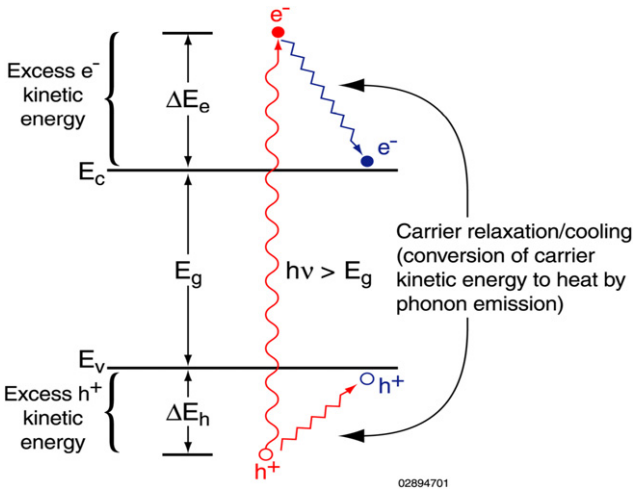

Fig. 1. Hot carrier relaxation/cooling in semiconductors (from Ref. [14]).

in laboratory-scale PV cells with two tandem p–n junctions, and a world-record 42.8% efficiency has been reported in a multi bandgap system at standard terrestrial conditions [15]. Although the tandem cell efficiencies are very impressive, their cost is very high.

Other approaches to exceed the Shockley–Queisser limit have been investigated. In 1978, it was first proposed that conversion efficiencies above 31% in single bandgap solar cells could be achieved by capturing the excess energy of e^-–h^+ pairs created by the absorption of solar photons larger than the bandgap to do useful work before these high-energy e^-–h^+ pairs convert their excess kinetic energy to heat through phonon emission [14,16–19]. This process is termed hot carrier conversion and produces higher photovoltages if the hot carriers can be captured by high-energy electron acceptors and/or donors, or by electrical contacts to the solar cell with appropriate work functions. In order to achieve the higher photovoltages, the rates of photogenerated carrier separation, transport, and interfacial transfer across the semiconductor interface must all be fast compared to the rate of carrier cooling [18–20].

To achieve higher photocurrent, the rate of e^-–h^+ pair multiplication (impact ionization (r_{II})) must be greater than the rates of carrier cooling ($r_{cooling}$), electron transfer (r_{ET}) of hot electrons, and the Auger recombination processes (r_{Auger}) (see Fig. 2.). Also, the rate of electron transfer of cooled electrons must be faster than the radiative recombination rate ($r_{radiative}$) and r_{Auger} [14,21].

Additional approaches to high efficiency have been proposed and studied and all approaches are commonly called 'third generation solar cells' [22]. Besides hot carrier solar cells [14,16–19], they include multiband and impurity band solar cells [22,23], thermophotovoltaic/thermophotonic cells [22], and up-and-down conversion of the incident solar photons [24,25].

2.2. PV with exciton multiplication

The detailed balance model of Shockley and Queisser has been used [26] to calculate the power conversion efficiency of single-gap and two-gap tandem solar conversion devices which employ QD absorbers capable of MEG after photon absorption. The results agree with previous calculations [27–31] on ideal solar cells with a single bandgap having greater than unity QY resulting from impact ionization.

MEG is incorporated into the calculations through the energy-dependent quantum yield, QY(E), for photon to carrier generation, which may exceed unity over certain photon energy ranges. The functional form for QY(E) to model the quantum yield for ideal MEG QD absorbers is given by a sum of step functions

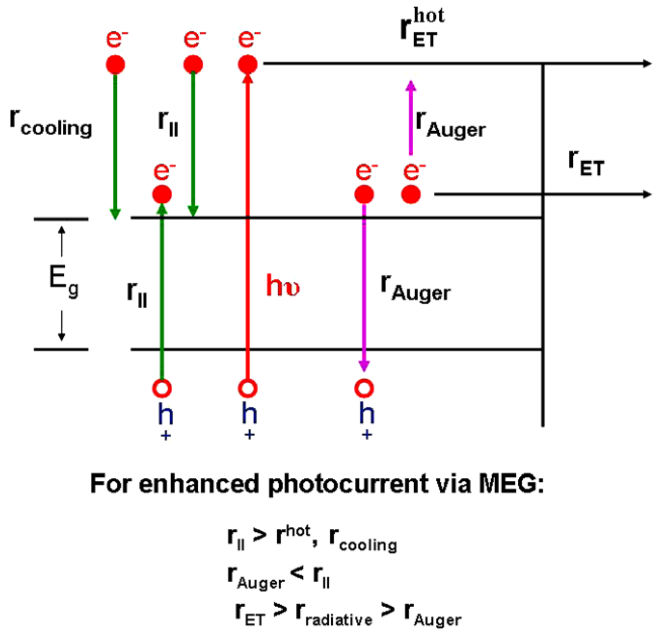

Fig. 2. Dynamical channels for photoinduced hot electron–hole pair.

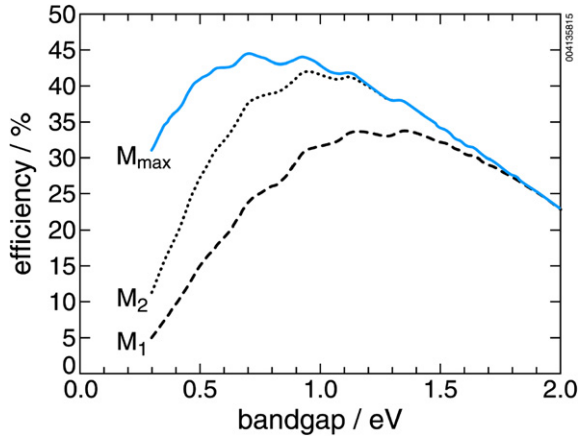

Fig. 3. Maximum thermodynamic power conversion efficiency with no solar concentration as a function of bandgap for different carrier multiplication values per photon absorbed (M). M_1 is the Shockley–Queisser result with 1 e^-–h^+ pair/photon, M_2 is the result for 2 e^-–h^+ pairs/photon, and M_{max} is the maximum multiplication possible from the solar spectrum. About 95% of the efficiency gain with carrier multiplication is obtained with generating just 2 e^-–h^+ pairs/photon.

$$QY(E) = \sum_{m=1}^{M} \theta(E, mE_g), \quad (1)$$

where θ (E,mE_g) is the Heaviside unit step function. Taking $M = 1$ gives the usual assumption of one e^-–h^+ pair generated per absorbed photon. Setting $M = M_{max} = E_{max}/E_g$ gives the maximum possible multiplication allowed by energetic constraints and the highest possible efficiency for a MEG device (i.e. M e^-–h^+ pairs for all photons that are M times E_g). We denote MEG absorbers with $M = 1$, $M = 2$, and $M = M_{max}$ as $M1$, $M2$, and M_{max}, respectively. The results are shown in Fig. 3.

3. Cooling dynamics in quantum dots

The rate of cooling of photoexcited excitonic states in semiconductor quantum dots compared to cooling through phonon emission controls the efficiency of exciton multiplication. Although rates of hot carrier cooling are very fast in bulk semiconductors (sub-ps time scale), the rates of excited state exciton cooling can be slowed down in quantized semiconductor structures because of the existence of discrete quantized energy levels. This arises because the energy separation between quantized levels in QDs can be many times the typical phonon energy, and in order for high-energy electrons and holes in higher excited quantized states in the QDs to cool by relaxing from a given quantum level to the next lower level, several phonons must be emitted simultaneously via electron–phonon scattering to satisfy energy conservation. This requires simultaneous multi-particle scattering events which become highly improbable with increasing numbers of phonons emitted. This effect is called a 'phonon bottleneck' and in experiments conducted with InP quantum dots the cooling time of hot electrons increased by about a factor of 10 (from 200–300 fs to 2–3 ps) if the Auger cooling channel was blocked, either by rapidly removing the photogenerated holes or avoiding their formation in the first place by injecting only electrons into the QDs [32]; photoexciting PbSe and PbS QDs, which have electrons and holes with equal effective masses, produces the same degree of slowed cooling by inhibiting the Auger cooling channel [38]. The slowed relaxation/cooling of hot excitons via phonon emission allow other channels for relaxation, such as MEG, to become competitive and even dominant in QDs.

4. Electron–hole pair (exciton) multiplication in quantum dots

Impact ionization (I.I.) cannot contribute to improved quantum yields in present solar cells based on Si, CdTe, $CuIn_xGa_{1-x}Se_2$, or III–V semiconductors because the maximum QY for I.I. does not exceed 1.0 until photon energies reach the ultraviolet region of the spectrum. In bulk semiconductors, the threshold photon energy for I.I. exceeds that required for energy conservation alone because, in addition to conserving energy, crystal momentum (**k**) must also be conserved. Additionally, the rate of I.I. must compete with the rate of energy relaxation by phonon emission through electron–phonon scattering. It has been shown that the rate of I.I. becomes competitive with phonon scattering rates only when the kinetic energy of the electron is many times the bandgap energy (E_g) [33–35]. The observed transition between inefficient and efficient I.I. occurs slowly; for example, in Si the I.I. efficiency was found to be only 5% (i.e. total quantum yield = 105%) at $h\nu \approx 4$ eV ($3.6E_g$), and 25% at $h\nu \approx 4.8$ eV ($4.4E_g$) [7,36]. This large blue shift of the threshold photon energy for I.I. in semiconductors prevents materials such as bulk Si and GaAs from yielding improved solar conversion efficiencies [9,36].

However, in quantum dots the rate of electron relaxation through electron–phonon interactions can be significantly reduced because of the discrete character of the e^-–h^+ spectra, and the rate of Auger processes, including the inverse Auger process of exciton multiplication, is greatly enhanced due to carrier confinement and the concomitantly increased e^-–h^+ Coulomb interaction. Furthermore, crystal momentum need not be conserved because momentum is not a good quantum number for three-dimensionally confined carriers (from the Heisenberg Uncertainty Principle the well-defined location of the electrons and holes in the nanocrystal makes the momentum uncertain). The concept of enhanced MEG in QDs is indicated in Fig. 4. Indeed, very efficient multiple e^-–h^+ pair (multi exciton) creation by one photon has now been reported in six semiconductor QD materials: PbSe, PbS, PbTe, CdSe, InAs, and Si, as described below.

Multi excitons have been detected using several spectroscopic measurements which are consistent with each other. The first method is to monitor the signature of multi exciton generation

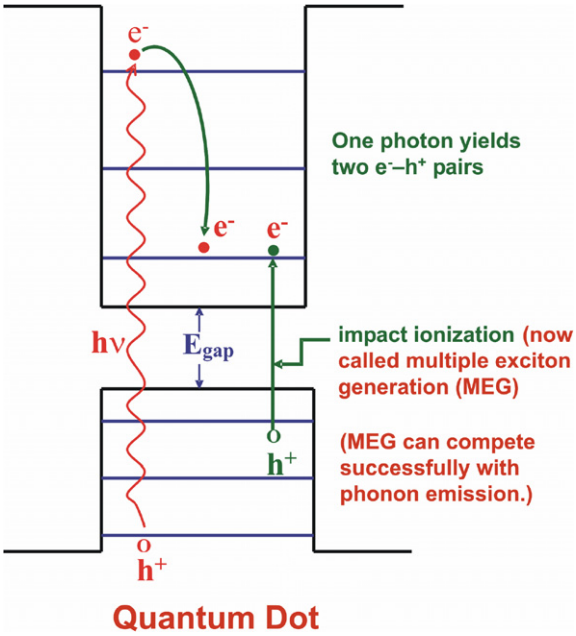

Fig. 4. Multiple electron–hole pair (exciton) generation (MEG) in quantum dots (from Ref. [21]).

using transient (pump–probe) absorption (TA) spectroscopy [37–41]. The multiple exciton analysis relies only on data for delays >5 ps, by which time carrier multiplication and cooling are complete and the probe pulse is interrogating the exciton population at their lowest state (the bandedges). In one type of TA experiment the probe pulse monitors the interband bleach dynamics with excitation across the QD bandgap; in a second type of experiment the probe pulse is in the mid-IR and monitors the intraband transitions (e.g. $1S_e$–$1P_e$) of the newly created excitons (see Fig. 5a). In the former case, the peak magnitude of the initial early time photoinduced absorption change created by the pump pulse plus the change in the Auger decay dynamics of the photogenerated excitons is related to the number of excitons created. In the latter case, the dynamics of the photoinduced mid-IR intraband absorption is monitored after the pump pulse (Fig. 5a). In Refs. [38,39], the transients are detected by probing either with a probe pulse exciting across the QD bandgap, or with a mid-IR probe pulse that monitors the first 1Se–1Sp intraband transition; both experiments yield the same MEG QYs.

When exciting a colloidal solution of NCs using a laser pulsewidth short compared to exciton recombination dynamics, the average number of photons absorbed per NC, $\langle N_0 \rangle$, can be calculated by the product of the absorption cross section, σ_a, and the pump photon fluence, j_p: $\langle N_0 \rangle = \sigma_a j_p$. The number of NCs that have absorbed m photons can be determined by the Poisson distribution function; $n_m = n_{NC} P(m)$, where $P(m) = \langle N_0 \rangle \exp(-\langle N_0 \rangle)/m!$ and n_{NC} is the concentration of NCs in the photoexcitation volume. For photon energies less the $2E_g$, only one exciton is produced per absorbed photon.

The first report of exciton multiplication was presented by Schaller and Klimov [37] for PbSe NCs; they reported an excitation energy threshold for the efficient formation of two excitons per photon at $3E_g$, where, E_g is the absorption energy gap of the nanocrystal (HOMO–LUMO transition energy) (it is common practice to refer to the HOMO–LUMO energy difference in QDs as the QD bandgap even though the electronic states are discrete). Schaller and Klimov reported a QY value of 218% (118% I.I. efficiency) at $3.8E_g$; QYs above 200% indicated the formation of more than two excitons per absorbed photon. The NREL research group reported [38] a QY value of 300% for 3.9 nm diameter PbSe QDs at a photon energy of $4E_g$, indicating the formation of three excitons per photon for every photoexcited QD in the sample. Evidence was also provided that the threshold energy for MEG by optical excitation is $2E_g$ [38], and it was shown that efficient MEG occurs also in PbS [38] (see Fig. 5b) and in PbTe nanocrystals [39].

In Ref. [38], the dependence of the MEG QY on the ratio of the pump photon energy to the bandgap (E_{hv}/E_g) varied from 1.9 to 5.0 for PbSe QD samples with $E_g = 0.72$ eV (dia. = 5.7 nm), $E_g = 0.82$ eV (dia. = 4.7 nm), and $E_g = 0.91$ eV (dia. = 3.9 nm), as shown in Fig. 5b. It was noted that the $2P_h$–$2P_e$ transition in the QDs is resonant with the $3E_g$ excitation, corresponding to the onset of sharply increasing MEG efficiency. This symmetric transition ($2P_h$–$2P_e$) dominates the absorption at $\sim 3E_g$, and the resulting excited state provides both the electron and the hole with excess energy of $1E_g$. A statistical analysis of these data also showed that the QY begins to surpass 1.0 at E_{hv}/E_g values greater than 2.0 (see Fig. 5b).

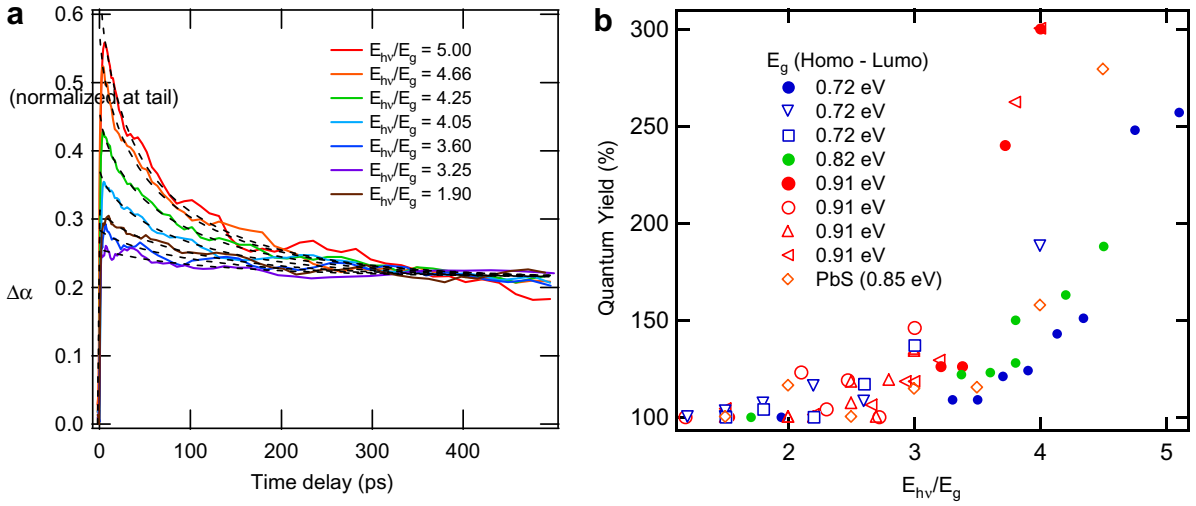

Fig. 5. (a) Exciton population decay dynamics obtained by probing intraband (intraexciton) transitions in the mid-IR at 5.0 μm for a sample of 5.7 nm diameter PbSe QDs. (b) QY for exciton formation from a single photon vs. photon energy expressed as the ratio of the photon energy to the QD bandgap (HOMO–LUMO energy) for three PbSe QD sizes and one PbS (dia. = 3.9, 4.7, 5.4 nm and 5.5 nm, respectively, and $E_g = 0.91$, 0.82, 0.73 eV, and 0.85 eV, respectively). Solid symbols indicate data acquired using mid-infrared probe; open symbols indicate bandedge probe energy. Quantum yield results were independent of the probe energy utilized (from Ref. [38]).

Additional experiments observing MEG have been reported for CdSe [40,42], PbTe [39], InAs [43,44], and Si [45]. In addition to TA, some of these optical experiments use time-resolved photoluminescence (TRPL) to monitor the effects of multi excitons on the PL decay dynamics, terahertz (THz) spectroscopy to probe the increased far infrared absorption of multi excitons, and quasi CW spectroscopy to observe the PL red shift and line shape changes due to multi excitons.

5. MEG in PbSe QD arrays

For high-efficiency in certain MEG QD solar cell designs, the QDs must be electronically coupled such that charge separation occurs on a timescale longer than MEG ($\sim 10^{-13}$ s) but shorter than the biexciton lifetime ($\sim 10^{-10}$ s). The separated charges must then drift and/or diffuse to the electrodes before recombining. In one potential device geometry [21], an ordered 3D QD film forms the intrinsic region of a p–i–n structure in which extended states, formed from the coupled QDs, allow for the delocalized photogenerated carriers to traverse the film and reach the contacts. Exchanging bulky capping ligands used in the QD synthesis with shorter molecules after film formation can drastically increase the carrier mobility of QD films [46–50] by reducing the interdot spacing [51] while retaining relatively highly-passivated surfaces. Distinct excitonic features are still evident in these electronically coupled QD arrays. While this type of close electronic coupling is necessary for the efficient extraction of carriers from a film, it is critical to determine if MEG is preserved in such QD films and to understand how the reduced quantum confinement of the excitons affects the MEG quantum yield (QY).

As for isolated QDs, the decay dynamics of single excitons in the QD films is first determined by photoexciting below the threshold energy for MEG (0.65 eV/810 nm), and then the films were excited above the threshold to obtain the information on exciton decay dynamics to determine the MEG QY. The determination of MEG using TA relies on the fact that multi exciton Auger recombination is much faster than single exciton recombination. A second, more simple analysis can be used [37,42,45,46] to deduce exciton generation efficiency. The ratio of the normalized change in transmission soon after the excitation pulse (3 ps) to that after all Auger recombination is complete (750 ps) is plotted versus photon fluence and the following equation can be fit to the data:

$$R_{\mathrm{pop}} = \frac{\left(\frac{\Delta T}{T_0}\right)_{t=3\mathrm{ps}}}{\left(\frac{\Delta T}{T_0}\right)_{t=750\mathrm{ps}}} = \frac{j_0 \cdot \sigma \cdot \mathrm{QY} \cdot \sigma}{1 - \exp(-j_0 \cdot \sigma)} \qquad (2)$$

where R_{pop} is defined as the ratio of exciton populations at 3 and 750 ps after excitation, J_0 is the photon fluence, σ is the absorbance cross section at the pump wavelength, QY is the number of excitons created per excited QD, and δ is the decrease in single exciton population over the time frame of the experiment (in this case, $e^{750-3(\mathrm{ps})/\tau_1}$). This analysis technique not only provides a reliable way to accurately determine the QY of exciton generation it also enables the direct determination of the absorption cross section (σ) of the QDs in the films at the pump wavelength without using a predetermined value, which may have some uncertainty.

Using this procedure the MEG efficiency was measured in an untreated and an electronically coupled film compared with that of a solution of QDs in TCE from the same synthesis (see Fig. 6). The QY can be obtained by calculating the ratio of the QY from the fits above and below the MEG threshold pumping conditions (see Fig. 6). In the sub-MEG threshold case, a fit of Eq. (2) (gray lines in Fig. 6) is applied where only σ and δ vary, and the QY is assumed to be 100%. Above the MEG threshold (green lines in Fig. 6), δ is fixed at its sub-MEG threshold value while the QY is allowed to vary. The best-fit value for the QY was found to be 148% at $\sim 4E_g$ for the QDs in TCE as well as in the untreated film, and corresponds to the overall average efficiency of exciton generation in an excited QD. The coupled film has an exciton generation efficiency of 164% at $\sim 4E_g$. This slight increase in the coupled film arises, to some extent, from the slightly lower E_g of the coupled film while using the same pump wavelength for all measurements. The QY for the films used in this work is plotted in Fig. 7 along with previously reported [38] values for PbSe QDs in solution versus energy gap multiple. The QY results for coupled QD films are similar to what has been previously reported for isolated dots suspended in solvents. These results were all repeated using a smaller size of QDs with larger E_g (0.90 eV) from another synthesis. The QY agrees well with the first sample, and the same trend is observed regarding single exciton and the biexciton lifetimes, aside from the biexciton lifetime scaling with volume.

Thus, after a post-film-fabrication soak treatment in 1 M hydrazine to electronically couple QDs in QD films, no reduction of MEG efficiency was found in the electronically coupled QD films compared to isolated QDs in solution. This is a particularly interesting and important result because one might expect that in QD arrays exhibiting appreciable electron delocalization resulting in reasonably good charge carrier transport, the MEG efficiency would be greatly reduced because of the reduction of quantum confinement. Thus, the ability to achieve effective electronic coupling between QDs in a QD film without reduction of MEG is very encouraging for the development of novel high-efficiency solar cells employing close-packed arrays of QDs. A related discovery presented below is

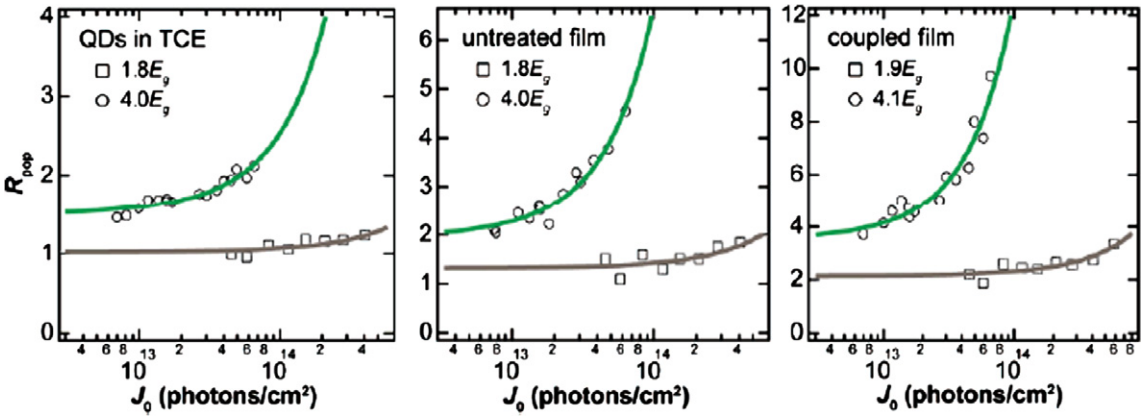

Fig. 6. Ratio of exciton population at 3–750 ps (R_{pop}) after excitation with pump energy of $<2E_g$ (squares) and $4E_g$ (circles) vs pump fluence for PbSe QDs in solution (left); in untreated PbSe QD films(middle); and in hydrazine-treated films (right). The fits to these data are described in the text (from Ref. [46]).

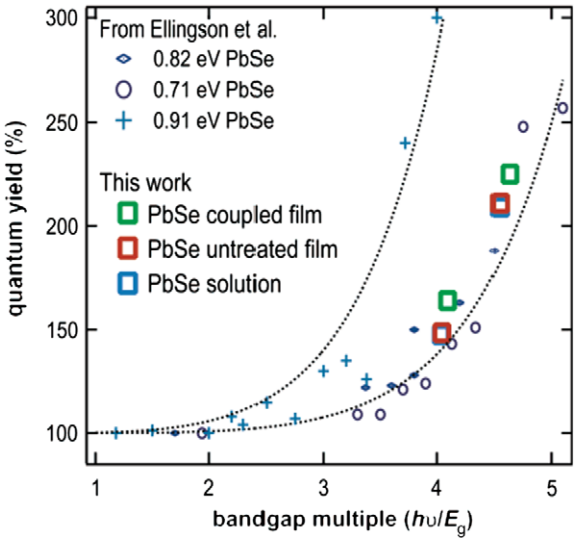

Fig. 7. Quantum yield of exciton generation for PbSe QD films and QD solutions. The dotted lines are guides to the eye. Note that the QYs for QDs in solution and untreated films are identical (from Ref. [46]).

that MEG can still be efficient in relatively large QDs of Si (5 nm radii, which is about equal to the Bohr radius if Si); this means that while the quantum confinement is not sufficient to produce a large confinement kinetic energy with an attendant large blue shift, the confinement is still enough to produce efficient MEG.

5.1. MEG in Si QDs

Silicon's indirect band structure yields extremely weak linear absorption at the bandgap, and thus one cannot readily probe a state-filling-induced bleach via this interband transition. Instead, the exciton population dynamics is probed by the method of photoinduced intraband absorption changes.

In Ref. [45], the first efficient MEG in Si NCs was reported using transient intraband absorption spectroscopy and the threshold photon energy for MEG was $2.4 \pm 0.1E_g$, and the quantum yield (QY) of excitons produced per absorbed photon reached 2.6 ± 0.2 at $3.4E_g$. In contrast, for bulk Si the threshold for impact ionization is $\sim 3.5E_g$ and the QY rises to only ~ 1.4 at $4.5E_g$ [36]. Highly efficient MEG in nanocrystalline Si at lower photon energies in the visible region has the potential to increase power conversion efficiency in Si-based PV cells toward a thermodynamic limit of $\sim$44% at standard AM1.5 solar intensity.

In the Si QD experiments, the probe was mainly at 0.86 eV, well below the effective bandgap. However, it was verified that the photoinduced absorption dynamics did not depend on the probe energy over a broad range from 0.28 to $\sim$1 eV. TA data below the threshold showed that the biexciton decay times for three different Si NC sizes depended linearly on the QD volume in agreement with the Auger recombination (AR) mechanism [52]. Thus, a new decay channel observed at high pump fluences was confirmed to be nonradiative AR.

When photoexciting above the energy conservation threshold for MEG ($>2E_g$) at low intensity, so that each photoexcited NC absorbs at most one photon, multi exciton AR serves as a metric for MEG. The amplitude of the AR component increases as the photon energy increases past the energy threshold for efficient MEG to occur. Fig. 8 shows the decay dynamics when $\langle N_0 \rangle$ is held constant at 0.5 at different pump wavelengths for the 9.5 nm and 3.8 nm samples, respectively. The black crosses are the decay dynamics for pump energies of 1.7 and $1.5E_g$ (below the MEG threshold) and the red crosses are for photon energies of 3.3 and $2.9E_g$ (above the MEG threshold). The data at long times (>300 ps) in Fig. 8 for the $3.3E_g$ pump are noisy, but the presence of the new fast decay component at times <300 ps is clearly evident. The data were modeled with only one adjustable parameter; the MEG efficiency, η.

By photoexciting above the energy conservation threshold for MEG ($>2E_g$) and at low intensity so that each photoexcited NC absorbs at most one photon, the appearance in Fig. 8 of fast multi exciton Auger recombination serves as a signature for MEG. No other alternative process other than MEG can be envisioned that is consistent with the following experimentally determined observations: (1) the dynamics are the same as AR (same decay rate and dependence on NC volume); (2) the PA amplitude steadily increases with photon energy with an onset greater than $2E_g$; and (3) it remains at low excitation fluences.

In addition to the TA experiments, MEG has been independently reported in the literature with two different PL measurements in CdSe [42] and InAs QDs [43]. Time-resolved photoluminescence (TRPL) single photon counting experiments measured both the dynamical signature of MEG, as in the TA experiments, as well as the biexciton PL spectrum under conditions where only one photon per NC is absorbed. A quasi-CW measurement also observed PL spectra indicative of the multi-excitonic state in InAs [43] NCs under conditions where absorption of more than one photon per NC is very improbable. For Si NCs, TRPL measurements are extremely challenging due to the long single exciton lifetimes relative to typical TRPL laser repetition rates (50–250 kHz) and the large difference between biexciton and single lifetimes which results in few photons being emitted within the biexciton lifetime. The quasi-

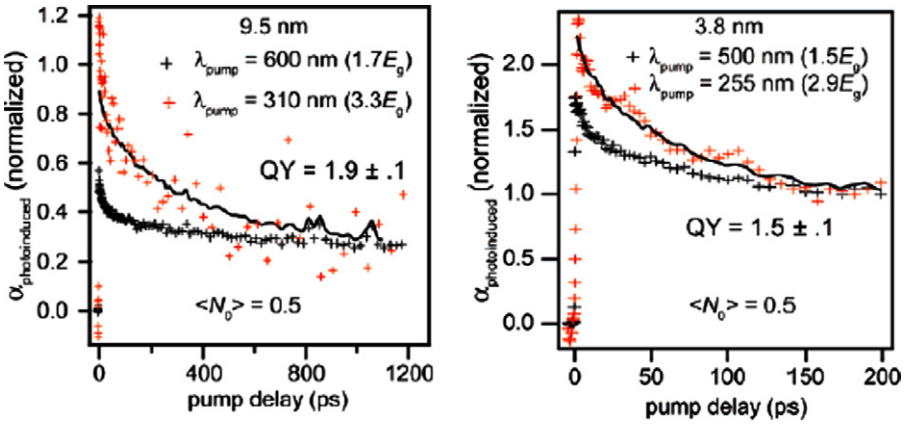

Fig. 8. Photoinduced transient absorption (TA) dynamics. Left: TA photoexciting below and above the MEG threshold for 9.5 nm Si QDs; Right: TA photoexciting below and above the MEG threshold for 3.8 nm Si QDs (from Ref. [45]).

CW method would also suffer from these limitations. TA measurements in Si NCs are complicated by the factor of ~100 to ~700 in the ratio of absorption cross sections for pump wavelengths below and above the MEG threshold. Hence the second method described above for PbSe QD films was invoked to acquire high quality QY data with high SNRs.

As previously described, in this second method the intensity dependence of the ratio of the exciton populations just after photoexcitation ($\tau > 0$) and after AR is complete ($\tau > 3t_2$) is determined, where τ is the pump–probe delay time and t_2 is the biexciton lifetime. It was reported [45] that for a 9.5 nm sample the y-axis intercept is 1.5 when exciting below $2E_g$, while the intercept is 2.9 for the case of $3.3E_g$ excitation; the analysis yields a QY of 1.9 ± 0.1, indicating very efficient MEG. The scatter in the data increases as the pump fluence decreases. However, fitting the data set to Eq. (2) but excluding the lowest two points does not change the value of the QY significantly (within the fitting error). Hence the scatter at low fluence does not increase the uncertainty of the derived QY values.

Fig. 9 presents the MEG QYs for Si QDs compared to literature data [36] for bulk Si obtained from photocurrent measurements in p–n junctions. The MEG QYs for Si QDs rise much more rapidly toward a QY of 3.0 at $3.5E_g$ and the threshold is at about $2.4E_g$; this is to be compared to a threshold of $3.5E_g$ for bulk Si and a QY of only 1.4 at $4.5E_g$. The best fit parameters have fitting errors of at most ~10% (for the 3.8 nm sample) and only ~5% for the 9.5 nm sample. In general, fitting Eq. (2) to each individual data set resulted in fitting errors that were smaller than the reproducibility. We estimate an onset of about $2.4E_g$ for MEG in Si QDs.

The exciton Bohr radius (a_B) for Si is 4.9 nm, which is about equal to the 9.5 nm diameter of the Si NCs. The very weak confinement regime is defined as $a > \sim 3a_B$ [53], and very strong confinement is defined as $a < a_B$; thus, 9.5 nm Si NCs are more appropriately characterized as being in the intermediate confinement regime and lack a large spectral blue shift. The present observation of efficient MEG in indirect-gap semiconductor NCs is an important result that has significance both for the theoretical model of MEG and for practical applications to solar photon conversion. This result implies that very strong confinement ($a \ll a_B$), as evidenced by a large blue-shift of the bandgap, is not necessary for efficient MEG, but only sufficient confinement is needed to produce stronger Coulomb coupling of the electrons and holes compared to the bulk, as discussed in Ref. [54]. Other theoretical models for MEG discussed below would have to be consistent with this important feature. The absence of the need for confinement that is sufficiently strong to produce a large blue-shift of the bandgap, means that the bandgap at which efficient MEG can occur lies close to the bulk bandgap. Si QDs with a diameter of 9.5 nm have a bandgap of 1.20 eV—only 80 meV larger than bulk Si—and shows efficient MEG. This bandgap is close to the optimum QD bandgap of 0.9–1.1 eV (see Fig. 3) for the highest possible PV efficiency of 42% utilizing cells with MEG yielding just two excitons per photon at a threshold of $2E_g$ [26]. However, to approach the highest possible PV efficiencies in actual solar cells, further research is needed to understand how to: (1) make the QY rise very steeply with photon energy after the MEG threshold; (2) establish the threshold as close as possible to $2E_g$; and (3) dissociate the excitons into free, separated electrons and holes, and collect them in the external circuit with a very high-efficiency.

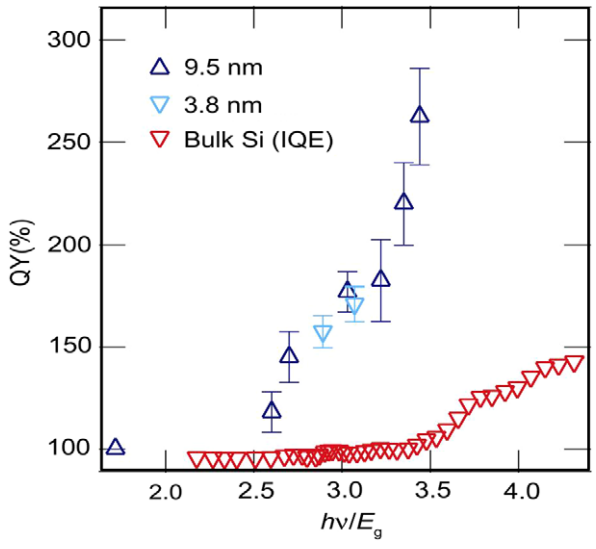

Fig. 9. MEG QY for 9.5 nm and 3.8 nm diameter Si QDs vs ratio of photon energy to QD bandgap (from Ref. [45]). Red triangles (inverted triangles) are data for bulk Si from Ref. [36].

6. Theory of MEG

Several theoretical models explaining the enhancement of MEG in quantum-confined NCs have been published, and disagreement remains [38,42,54–56]. Many of these models depend upon enhanced Coulomb coupling in the QDs. In a novel theory of MEG [54], efficient MEG by a single photon in NCs is explained by the formation of a coherent superposition of single and multi exciton states (see Fig. 10). The model uses a time-dependent density matrix approach, which allows simultaneous consideration of an arbitrary strength of coupling between single and multi exciton states, different dephasing rates for these states, and short pulse excitation of the NCs. The steady-state solution of the density matrix equations yields the following conditions for efficient MEG: (1) the energy relaxation rate of a single exciton (γ_1) initiated by light must be slower than both the energy relaxation rate of the multi exciton (γ_2) and the rate of Coulomb coupling between the two states ($W_C/\hbar$), where, W_C is the matrix element of the Coulomb interaction between the single and multi exciton states

$$W_C = \langle \Psi_{1Ex} | e^2/\varepsilon \mathbf{r} | \Psi_{nEx} \rangle \quad (3)$$

and Ψ_{1Ex} is the initial single exciton state, Ψ_{nEx} is the multi exciton state, ε is the dielectric constant in the QD, and $\mathbf{r}$ is the vectorial distance between the electronic particles in the QD. The density matrix approach is the only self-consistent method that takes into account the diverse processes responsible for MEG in NCs.

Under optical excitation of NCs, a single photon can only generate a single electron–hole pair which is not an eigenstate of the multielectron Hamiltonian that describes the superposition of multi excitons. This initial single e^-–h^+ pair state (exciton) is coupled with the multi exciton states and creates a superposition of single and multi excitons. The theory has been applied to PbSe NCs where the onset of very efficient MEG occurs at photon energies of $3E_g$ corresponding to a $2P_h$ to $2P_e$ transition [54] (but note that the threshold for the onset of (weak) MEG is $2E_g$).

For a strongly coupled superposition of single and multi exciton states, the question of MEG efficiency is reduced to the question of the state relaxation. The single and multi exciton components of the superposition have different decay rates, and the ratio of these rates determines what a single photon creates: a single exciton or multi excitons.

To calculate the efficiency of MEG, it is necessary to compare the populations of the ground biexcitons, N_{bi}, to the single exciton, N_{ex}, during time, t, which is much longer than the relaxation times of the excited states ($1/\gamma_1$ and $1/\gamma_2$, respectively) but much shorter than the lifetime of the bandedge excitons ($1/\Gamma_{ex}$ and $1/\Gamma_{bi}$); i.e. $1/\gamma_1 \leqslant 1/\gamma_2 \ll 1/\Gamma_{bi} \ll 1/\Gamma_{ex}$. This approach ultimately yielded the ratio of the bandedge biexciton and single exciton populations [54]:

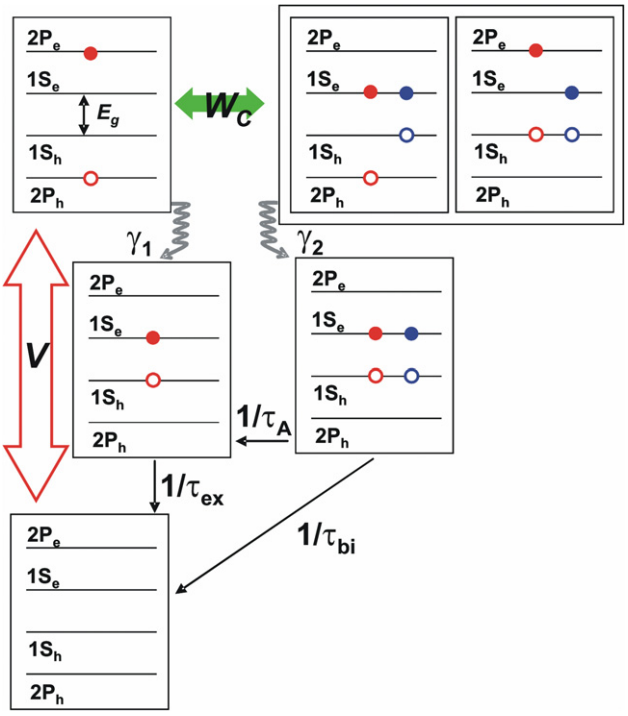

Fig. 10. Theoretical model for MEG. For simplicity, only 3 degenerate states are shown upon absorption of a $3E_g$ photon ($2P_h$–$2P_e$): the initial single $2P_h2P_e$ exciton, and the two excited biexciton states ($2P_h1S_e1S_h1S_e$, $1S_h1S_e2P_e1S_e$). For simplicity, the 4th state ($1S_h1S_e1S_h1S_e1S_h1S_e$) is not represented and electronic states between the 1S and 2P states are also not shown. The 3 degenerate states are coupled by the Coulomb interaction (W_C) and form a coherent superposition of 3 states; their populations experience oscillations with time (quantum beats). The relaxation (cooling) rate of the single exciton state ($1/\gamma_1$) is slower than the relaxation rate of the biexciton states ($1/\gamma_2$) because of the asymmetric charge distribution in the excited biexcitons (the latter enhances electron–phonon coupling). This preferential dephasing of the coherence for the excited biexcitons results in the final formation of a biexciton from a single photon. V is the overall rate of decay of the excited single exciton to the ground state, while $1/\tau_{ex}$ and $1/\tau_{bi}$ are the rates of the decay of the relaxed (cooled) single exciton and biexcitons to the ground state. All of these latter 3 rates are slow compared to the rates of relaxation and Coulomb coupling (from Ref. [57]).

$$N_{bi}/N_{ex} = (\gamma_2/\gamma_1)P_{1-2} \quad (4)$$

where P_{1-2} is the probability of the population of the excited biexciton state via its Coulomb coupling to the single exciton state excited by a photon; its value is always <1.

Eq. (4) shows that efficient MEG, i.e. the predominant generation of multi excitons, is possible only if the relaxation rate of the biexciton is much faster than that of the exciton ($\gamma_2 \gg \gamma_1$), because $P_{1-2} < 1$. For strong coupling, the transition probability approaches 1 and the population ratio approaches its maximum value of (γ_2/γ_1).

MEG, however, can be efficient even for a weak coupling regime, $W_C/\hbar \ll \gamma_2$. In this case, $N_{bi}/N_{ex} = 4W_C^2/(\hbar^2\ \gamma_1\ \gamma_2)$, and can be much larger than unity if $W_C/\hbar \gg \gamma_1$ [54]. The relative population N_{bi}/N_{ex} is then determined by the ratio of the biexciton creation rate, $(2W_C/\hbar)^2\ \gamma_2$, to the direct single exciton relaxation rate, γ_1. Detuning of the resonance between single and multi exciton states, for example from a significant size dispersion of the NC population, slows down the formation of a coherent superposition.

It was found theoretically [54] that the biexciton relaxation rate is much faster than the single exciton relaxation rate, assuming that the relaxation rate for various e^-–h^+ pair configurations is proportional to their coupling with phonons. These calculations show that polar interactions of intrinsic semiconductor phonons in CdSe and PbSe NCs with asymmetric e–h pair configuration are 10 to 40 times stronger than that of their coupling with symmetric e^-–h^+ pair configurations (nL_enL_h). This is because in the latter case, charge distributions of the optically created electron and hole compensate each other almost exactly at each point of the NC, and the NC thus retains its local neutrality even after exciton creation. As a result, exciton interactions with the polar optical phonons that are sensing the total charge are very weak [58]. It also is quite obvious that the coupling of asymmetric e–h configurations with phonons of organic molecules at the NC surface [59] should be significantly stronger as well. In both cases, weak coupling of symmetric e^-–h^+ pairs created by light with phonons suppresses their relaxation and would result in efficient MEG because the condition $\gamma_1 \ll \gamma_2$ is fulfilled.

Theoretically, the MEG QY will not show a size dependence if it is assumed that the ratio γ_1/γ_2 does not depend on size. At the same time, an increase of γ_2/γ_1 always leads to an increase of QY. The predicted size independence of the average number of e^-–h^+ pairs generated via excitation of the same optical transition is consistent with experimental results [37–39,41], which show that the QY depends only weakly on size and is a function primarily of only one parameter: $E_{h\nu}/E_g$.

In conclusion, a mechanism for MEG was introduced in Ref. [54] that invokes a coherent superposition of multiple excitonic states, meaning that multiple excitons are essentially created extremely fast upon absorption of high-energy photons [38,54]; this new model also explains the lower threshold photon energy for MEG at $2E_g$.

7. MEG photocurrent

To date, all reports published on observing MEG in QDs have been based on spectroscopic measurements, where the MEG QY is determined by analyzing the effects of the formation of multiple excitons on light. Although, as discussed above, there have been several different types of spectroscopic measurements (transient interband bleaching probed with bandgap excitation, transient intraband photoinduced absorption in the mid-IR, transient THz spectroscopy, time-resolved photoluminescence, and quasi-CW photoluminescence spectroscopy) and they all report results on MEG with six different semiconductors that are consistent with one other, all these spectroscopic measurement are nevertheless indirect methods of measuring MEG. The most direct method for determining how many e^-–h^+ pairs are created per absorbed photon is to count the electrons in photocurrent measured in an external circuit connected to an optoelectronic device consisting of QDs where light is absorbed only in the QDs. If the measured QY for the photocurrent is >1.0, then there can be no doubt whatsoever that MEG is occurring within the QDs. This result requires that in the QD device the time scale for exciton dissociation, charge separation, and charge transport be much faster compared to exciton or separated e^-–h^+ pair recombination.

The most convincing result would be a measurement of a QY > 1.0 with respect to the incident photon flux (defined as the external QY (EQY)). However, in all optoelectronic QD devices, when the QDs are configured to allow charge extraction of the dissociated excitons, new and efficient non-radiative recombination channels are opened that arise from the charge delocalization and attendant greatly increased density of surface trapping and recombination sites. An EQY > 1.0 would require that the other losses in the device, such as reflection, transmission, scattering, re-radiation, and absorption in the non-QD elements of the device structure added to the new non-radiative recombination channels arising from charge collection do not exceed the increase in exciton population created through MEG. The latter loses could be accounted for by measuring the QY for photocurrent based only on the photon flux absorbed in the QDs (this is defined as the internal

QY (IQY)). But the IQY requires knowledge of the optical and dielectric constants of the heterogeneous QD device, which is difficult to obtain accurately. As a result, to date no photocurrent measurements from QD device structures show an EQY or an IQY with a QY > 1.0. Many research groups are working on this problem and some promising advances in device architecture have been made [60,61] that may allow a definitive determination of whether the EQY or IQY for photocurrent is >1.0.

8. Controversial aspects of MEG

Besides the lack of published reports of an EQY or IQY > 1.0 for photocurrent extracted from optoelectronic QD devices (as discussed above), another recently reported result [62] that has raised some concern about MEG is that the TRPL measurements of exciton multiplication in CdSe and CdTe QDs reported in Ref. [42] cannot be reproduced. In Ref. [62], the authors find no change in the PL decay dynamics upon excitation with $>3E_g$ photons compared to photons with energy $<2E_g$. However, the excitation energy for the experiments with CdSe and CdTe QDs require rather energetic photons (>5.5 eV) that may induce the involvement of surface species in the QD excited state decay dynamics. Experiments by the authors of Ref. [42] to explain the discrepancy in the TRPL results are in progress.

Note added in proof

The authors of Ref. [43] report that they cannot repeat their THz results with their same InAs QDs [63,64] also report they find no MEG in InAs core-shell QDs using TA. It appears from these reports and Ref. [62] that for some QD materials MEG efficiencies may depend upon their specific surface chemistry.

Acknowledgments

This review is based on the work of the NREL team (Matt Beard, Randy Ellingson, Joey Luther, Matt Law, Mark Hanna, Justin Johnson, Jim Murphy, Pingrong Yu, Qing Song) and theorists at the Naval Research Laboratory (Alexander L. Efros and Andrew Shabaev), and the publications they co-authored and cited here. We acknowledge the support of the US. Department of Energy, Office of Science, Office of Basic Energy Sciences, Division of Chemical Sciences, Biosciences and Geosciences under Contract No. DEAC36-99GO10337 to NREL.

References

[1] A.J. Nozik, R. Memming, J. Phys. Chem. 100 (1996) 13061.
[2] R. Memming, Semiconductor Electrochemistry, Wiley-VCH, Weinheim, 2002.
[3] S. Koc, Czech. J. Phys. 7 (1957) 91.
[4] V.S. Vavilov, J. Phys. Chem. Solids 8 (1959) 223.
[5] J. Tauc, J. Phys. Chem. Solids 8 (1959) 219.
[6] V.N. Ivakhno, Sov. Phys. Solid State 14 (1972) 481.
[7] O. Christensen, J. Appl. Phys. 47 (1976) 689.
[8] A.R. Beattie, J. Phys. Chem. Solids 24 (1962) 1049.
[9] S. Kolodinski, J.H. Werner, T. Wittchen, H.J. Queisser, Appl. Phys. Lett. 63 (1993) 2405.
[10] N.S. Baryshev, M.P. Shchetinin, S.P. Chashchin, Y.S. Kharionovskii, I.S. Aver'yanov, Sov. Phys. Semicond. 8 (1974) 192.
[11] W. Shockley, H.J. Queisser, J. Appl. Phys. 32 (1961) 510.
[12] R.T. Ross, J. Chem. Phys. 45 (1966) 1.
[13] R.T. Ross, J. Chem. Phys. 46 (1967) 4590.
[14] A.J. Nozik, Annu. Rev. Phys. Chem. 52 (2001) 193.
[15] Press Release, University of Delaware, July 23, 2007.
[16] F. Williams, A.J. Nozik, Nature 271 (1978) 137.
[17] R.T. Ross, A.J. Nozik, J. Appl. Phys. 53 (1982) 3813.
[18] D.S. Boudreaux, F. Williams, A.J. Nozik, J. Appl. Phys. 51 (1980) 2158.
[19] F.E. Williams, A.J. Nozik, Nature 311 (1984) 21.
[20] A.J. Nozik, Philos. Trans. R. Soc. London Ser. A A295 (1980) 453.
[21] A.J. Nozik, Physica E 14 (2002) 115.
[22] M.A. Green, Third Generation Photovoltaics, Bridge Printery, Sydney, 2001.
[23] A. Luque, A. Martí, Phys. Rev. Lett. 78 (1997) 5014.
[24] T. Trupke, M.A. Green, P. Würfel, J. Appl. Phys. 92 (2002) 4117.
[25] T. Trupke, M.A. Green, P. Würfel, J. Appl. Phys. 92 (2002) 1668.
[26] M.C. Hanna, A.J. Nozik, J. Appl. Phys. 100 (2006) 074510.
[27] J.H. Werner, S. Kolodinski, H.J. Queisser, Phys. Rev. Lett. 72 (1994) 3851.
[28] W. Spirkl, H. Ries, Phys. Rev. B 52 (1995) 11319.
[29] R. Brendel, J.H. Werner, H.J. Queisser, Sol. Energy Mat. Sol. Cells 41-2 (1996) 419.
[30] A. De Vos, B. Desoete, Sol. Energy Mater. Sol. Cells 51 (1998) 413.
[31] P.T. Landsberg, V. Badescu, J. Phys. D: Appl. Phys. 35 (2002) 1236.
[32] J.L. Blackburn, R.J. Ellingson, O.I. Mićić, A.J. Nozik, J. Phys. Chem. B 107 (2003) 102.
[33] J. Bude, K. Hess, J. Appl. Phys. 72 (1992) 3554.
[34] H.K. Jung, K. Taniguchi, C. Hamaguchi, J. Appl. Phys. 79 (1996) 2473.
[35] D. Harrison, R.A. Abram, S. Brand, J. Appl. Phys. 85 (1999) 8186.
[36] M. Wolf, R. Brendel, J.H. Werner, H.J. Queisser, J. Appl. Phys. 83 (1998) 4213.
[37] R. Schaller, V. Klimov, Phys. Rev. Lett. 92 (2004) 186601.
[38] R.J. Ellingson et al., Nano Lett. 5 (2005) 865.
[39] J.E. Murphy et al., J. Am. Chem. Soc. 128 (2006) 3241.
[40] R.D. Schaller, M.A. Petruska, V.I. Klimov, Appl. Phys. Lett. 87 (2005) 253102.
[41] R.D. Schaller, M. Sykora, J.M. Pietryga, V.I. Klimov, Nano Lett. 6 (2006) 424.
[42] R.D. Schaller, M. Sykora, S. Jeong, V.I. Klimov, J. Phys. Chem. B 110 (2006) 25332.
[43] J.J.H. Pijpers et al., J. Phys. Chem. C 111 (2007) 4146.
[44] R.D. Schaller, J.M. Pietryga, V.I. Klimov, Nano Lett. 7 (2007) 3469.
[45] M.C. Beard et al., Nano Lett. 7 (2007) 2506.
[46] J.E. Murphy, M.C. Beard, A.J. Nozik, J. Phys. Chem. B 110 (2006) 25455.
[47] D.V. Talapin, C.B. Murray, Science 310 (2005) 86.
[48] B.L. Wehrenberg, D. Yu, J.S. Ma, P. Guyot-Sionnest, J. Phys. Chem. B 109 (2005) 20192.
[49] B.L. Wehrenberg, P. Guyot-Sionnest, J. Am. Chem. Soc. 125 (2003) 7806.
[50] D. Yu, C.J. Wang, P. Guyot-Sionnest, Science 300 (2003) 1277.
[51] J.J. Urban, D.V. Talapin, E.V. Shevchenko, C.B. Murray, J. Am. Chem. Soc. 128 (2006) 3248.
[52] D. Kovalev, J. Diener, H. Heckler, G. Polisski, N. Kunzner, F. Koch, Phys. Rev. B 61 (2000) 4485.
[53] A.L. Efros, in: A.L. Efros, D.J. Lockwood, L. Tsybeskov (Eds.), Semiconductor Nanocrystals: from Basic Principles to Applications, Kluwer Academic/Plenum Publishers, New York, 2003, p. 52.
[54] A. Shabaev, A.L. Efros, A.J. Nozik, Nano Lett. 6 (2006) 2856.
[55] R.D. Schaller, V.M. Agranovich, V.I. Klimov, Nat. Phys. 1 (2005) 189.
[56] A. Franceschetti, J.M. An, A. Zunger, Nano Lett. 6 (2006) 2191.
[57] A.L. Efros, A. Shabaev, private communication.
[58] S. Schmitt-Rink, D.A.B. Miller, D.C. Chemla, Phys. Rev. B 35 (1987) 8113.
[59] P. Guyot-Sionnest, B. Wehrenberg, D. Yu, J. Chem. Phys. 123 (2005) 074709.
[60] J.M. Luther, M. Law, Q. Song, C.L. Perkins, M.C. Beard, A.J. Nozik, ACS Nano 2 (2008) 271.
[61] J. M. Luther, Thesis, Colorado School of Mines, 2007.
[62] G. Nair, M.G. Bawendi, Phys. Rev. B 76 (2007) 081304(R).
[63] J.J.H. Pijpers et al., J. Phys. Chem. (2008), in press.
[64] M. Ben-LuLu et al., Nano Lett. (2008), in press.

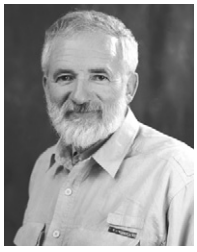

Dr. Arthur J. Nozik is a Senior Research Fellow at the U.S. DOE National Renewable Energy Laboratory (NREL) and Professor Adjoint in the Department of Chemistry and Biochemistry at the University of Colorado, Boulder. In 2007 he was appointed the Scientific Director of the new Center for Revolutionary Solar Photoconversion under the Colorado Renewable Energy Collaboratory. Nozik received his BChE from Cornell University in 1959 and his PhD in Physical Chemistry from Yale University in 1967. Before joining NREL in 1978, then known as the Solar Energy Research Institute (SERI), he conducted research at the Materials Research Center of the Allied Chemical Corporation (now Honeywell, Inc). Dr. Nozik's research interests include size quantization effects in semiconductor quantum dots and quantum wells, including multiple exciton generation from a single photon; the applications of unique effects in nanostructures to advanced approaches for solar photon conversion; photogenerated carrier relaxation dynamics in various semiconductor structures; photoelectrochemistry of semiconductor-molecule interfaces; photoelectrochemical energy conversion; photocatalysis; optical, magnetic and electrical properties of solids; and Mössbauer spectroscopy. He has published over 200 papers and book chapters in these fields, written or edited 5 books, holds 11 U.S. patents, and has delivered over 250 invited talks at universities, conferences, and symposia. He has served on numerous scientific review and advisory panels, chaired and organized many international and national conferences, workshops, and symposia, and received several awards in solar energy research, including the 2008 Eni Award and the 2002 Research Award of the Electrochemical Society. Dr. Nozik has been a Senior Editor of The Journal of Physical Chemistry from 1993 to 2005. A Special Festschrift Issue of The Journal of Physical Chemistry honoring Dr. Nozik's scientific career appeared in the December 21, 2006 issue. Dr. Nozik is a Fellow of the American Physical Society and a Fellow of the American Association for the Advancement of Science; he is also a member of the American Chemical Society, the Electrochemical Society, and the Materials Research Society.